POAC'15
Trondheim, Norway

Proceedings of the 23rd International Conference on
Port and Ocean Engineering under Arctic Conditions
June 14-18, 2015
Trondheim, Norway

MARINE ICING OBSERVED ON KV NORDKAPP DURING A COLD AIR OUTBREAK WITH A DEVELOPING POLAR LOW IN THE BARENTS SEA

[1,2]Samuelsen, E. M., Løset, S.[3,4] and Edvardsen, K.[1]

[1]UiT - The Arctic University of Norway, NO-9037 Tromsø, Norway

[2]MET Norway - Norwegian Meteorological Institute, Tromsø, Norway

[3]Sustainable Arctic Marine and Coastal Technology (SAMCoT), Centre for Research-Based Innovation (CRI), Norwegian University of Science and Technology, Trondheim, Norway

[4]The University Centre in Svalbard, UNIS, Norway

ABSTRACT

Marine icing is a phenomenon that may occur for temperatures below subfreezing where sea spray either is lofted from the sea surface or being generated by waves interacting with a ship or a structure. On a voyage from Tromsø to the waters east of Bjørnøya late February 1987, the Norwegian Coast Guard vessel KV Nordkapp experienced heavy icing due to a polar low that raged over these waters during the voyage. This polar low developed in an unstable air mass due to a cold-air outbreak over relatively warm waters. KV Nordkapp experienced air temperatures in the range of -10°C to -20°C, and was moving against 20-30 m/s winds producing waves up to 7.5 m high. During the icing event KV Nordkapp accumulated 110 tons of ice. The icing was encountered all the way from the hull just above the water level to the top of the wheelhouse. The icing event is analysed and calculations made for comparison between observations and modelling results.

Keywords: Arctic, Marine icing, Polar low

INTRODUCTION

Icing on ships is a major safety concern as the weight of the ice affects both the ship's stability and manoeuvrability, and has caused numerous accidents and shipwrecking (Shellard, 1974). During the last 40 years this has been a motivation for the maritime research community to develop forecasting algorithms for icing (Kachurin et al., 1974; Stallabrass, 1980; Overland et al., 1986; Makkonen, 1987; Horjen, 1990; Henry, 1995; Lozowski et al., 2000), trying to calculate the icing rate by solving the heat equation (eq. 1) of a freezing surface. Also a model based on Computational Fluid Dynamics (CFD) calculations, has recently been developed (Kulyakhtin, 2014) which simulates the local air stream and icing rate, taking into account the more complete geometry of the whole ship or structure. On the northern hemisphere, the Barents Sea is especially exposed to severe marine icing (Jørgensen, 1981), therefore reliable icing forecasts are desirable. Only a few algorithms have been adapted by the meteorological society (Ekeberg, 2010), and today the Overland (1990) algorithm is the most widely used among the Norwegian weather forecasters (Survey among Operational weather forecasters at MET Norway, Tromsø, 2014, pers. comm., March). The model has been criticized for

Table 1: List of symbols, expressions and values used in the paper and inside the calculations when nothing else is stated.

Symbol	Description	Value/Expression	Units	Comments
a_0	Coeff. in front of v in h_a used in Overland algorithms	62	$Ws/m^3°C$	The value refer to O3 algorithm
$Bias$	Mean error	$\frac{1}{n'}\sum_{i=1}^{n'}(P_i - O_i)$		P_i predicted value, O_i observed value
c	Wave phase speed	eq.5 (p.8)	m/s	
c_{dir}	Wave direction		°	Assumed to be equal to DD
c_p	Specific heat capacity of air at const. pressure	1004	$J/kg°C$	
c_w	Specific heat capacity of water	4000	$J/kg°C$	
D	Freezing plate dimension	4	m	Width of plate on KV Nordkapp
DD	Wind direction		°	Az. ang. where wind is blowing from
Dir	Ship direction		°	Az. ang. where boat is coming from
D_p	Water depth		m	
d	Water droplet diameter	0.002	m	Taken from Stallabrass (1980)
E	Collection efficiency	$E = \frac{\zeta-2800}{\zeta+11700}, \zeta \geq 2800, \zeta = \frac{v_d^{0.6}(d\times10^6)^{1.6}}{D}$		Stallabrass (1980)
$e_s(T)$	Saturation vapour pressure for a given temperature, T (°C)	$6.112\times\exp(\frac{17.67T}{T+243.5})$	hPa	Bolton (1980)
g	Gravitational acceleration	9.81	m/s^2	
h	Ice thickness		cm	
$\frac{dh}{dt}$	Ice accretion rate		cm/h	
$\sum h$	Total accumulated ice in time period		cm	
h_a	Heat transfer coefficient	$\frac{k_a Nu}{D} = 6.4\times\frac{W_r^{0.8}}{D^{0.2}} = 4.85W_r^{0.8}$	$W/m^2°C$	W_r used to represent air stream velocity.
h_e	Evaporative heat transfer coefficient	$1.12h_a\frac{\varepsilon L_v}{c_p p} = 1739\frac{h_a}{p}$	$W/m^2°C$	
H_s	Significant wave height		m	
k^*	Interfacial distribution coeff., i.e. ratio of entrapped water inside ice when freezing.	0.3		Makkonen (1987, 2010)
k_a	Heat capacity of air	0.023	W/m°C	
L_f	Latent heat of freezing for pure ice	3.33×10^5	J/kg	
L_{fs}	Latent heat of freezing for saline ice	$(1-k^*)L_f = 2.33\times10^5$	J/kg	
L_v	Latent heat of vaporization of water	2.5×10^6	J/kg	
lwc	Liquid water content in spray	$w_0 H_s \times V_r^2 \exp(-0.55z)$	kg/m^3	Zakrzewski (1987), slightly corrected constant
MAE	Mean absolute error	$\frac{1}{n'}\sum_{i=1}^{n'}\lvert P_i - O_i\rvert$		P_i predicted value, O_i observed value
n	Freezing fraction	$\frac{R_i}{R_w}$		
N	Spray frequency	$60^{-1}(15.78 - 18.04\times\exp(\frac{-4.26}{t_{per}}))$	s^{-1}	Zakrzewski (1986, 1987), $15 \geq t_{per} \geq 3.5s$
Nu	Nusselt number	$0.0322\times Re^{0.8}$		Rectangular shaped body in turb. flow (Stallabrass, 1980)
Nu_d	Droplet nusselt number	$0.37Re^{0.6} = 23$		Stallabrass (1980)
Pr	Predictor in Overland algorithm	see eq.2 (p.4)		
P_w	Significant wave period		s	
p	Pressure at mean sea level		hPa	
Q_c	Convective heat flux, i.e. the cooling of the surface from the air temperature	$h_a\times(T_s - T_a)$	W/m^2	
Q_d	Warming or cooling of the freezing surface by the impinging sea water	$R_w c_w \times (T_s - T_d)$	W/m^2	
Q_e	Evaporative heat flux, i.e. the evaporative cooling of the surface from the air	$h_e\times(e_s(T_s) - RH\times e_s(T_a))$	W/m^2	
Q_f	Heat flux released by freezing	$L_{fs}R_i$	W/m^2	
Re	Reynolds number	$\frac{vD}{\nu}$		
RH	Relative humidity of the air		%	RH is used as a fraction in calculations
R_i	Ice accretion flux	$\rho_i\frac{dh}{dt}$	kg/m^2s	
R_w	Sea spray flux	$v_d E\times lwc\times t_{dur}N$	kg/m^2s	Time averaged spray flux
S_b	Salinity of freezing brine	$S_b = \frac{S_w}{1-n\times(1-k^*)}$	ppt	Makkonen (1987)
S_w	Salinity of impinging sea water		ppt	
SST	Sea surface temperature		°C	
s	Distance from edge of ship to icing plate	eq. 6 (p.8)	m	
s_r	Distance of droplet movement using α_c in eq. 6 (p.8)		m	
T_a	Air temperature		°C	
T_d	Temperature of incoming sea water droplets		°C	
T_{dew}	Dew-point temperature of air		°C	
T_f	Freezing point of sea water	$-0.002 - 0.0524\times S_w - 6\times10^{-5}\times S_w^2$	°C	Stallabrass (1980), S_w in ppt
T_s	Temperature of freezing surface		°C	
Δt	Droplet cooling time	$\tau + t_{dur}/2$	s	Average cooling time of droplets in air.
$t_{durtotal}$	Duration of spray cloud of whole ship	$\frac{10V_r H_s}{v^2}$	s	Lozowski et al. (2000) for USCGC Midgett (115 m long)
t_{dur}	Duration of spray cloud at a certain position of ship	$t_{durtotal} - \tau$	s	Zakrzewski (1987)
t_{per}	Period between collisions	$\frac{cP_w}{V_r}$	s	Zakrzewski (1987)
v	Wind speed		m/s	Measured at around 22 mASL on KV Nordkapp
v_d	Droplet velocity		m/s	Assumed to be equal to W_r
V_r	Relative velocity between waves and boat	$c - v_s\cos(\alpha)$	m/s	Aksyutin (1979)
v_s	Boat speed		m/s	
w_0	Const. in lwc formulation	6.36×10^{-5}		Zakrzewski (1987), slightly corrected constant
W_r	Relative velocity between wind and boat	$\sqrt{v^2 + v_s^2 - 2v_s v\cos(\alpha)}$	m/s	
z	Height above deck level of a medium sized fishing vessel (MFV)		m	Starts approx. 3.5 m above sea level
α	Angle between wind vector and ship	$DD - Dir$	°	
α_c	Angle between relative wind vector and ship	$180° - \arcsin(\frac{v\sin(\alpha)}{W_r})$	°	Taken from Zakrzewski et al. (1988)
ε	Ratio of molecular weights of water and air	0.622		
λ	Wave length	cP_w	m	
ρ_i	Density of sea ice	890	kg/m^3	Taken from Stallabrass (1980)
ρ_w	Density of sea water	1028	kg/m^3	
ν	Kinematic viscosity	1.2×10^{-5}	m^2/s	
τ	Droplet flight time	$\frac{s_r}{W_r}$	s	Assuming droplets move at const. W_r from same init. pos.

being partly non-physical, and too sensitive to low sea-surface temperatures (Makkonen et al., 1991), but still it has been used in a newer climatology study of icing (Moore, 2013). The Canadian weather

service has implemented another algorithm based on the Stallabrass (1980) algorithm (Henry, 1995). It is often referred to as the Modified Stallabrass (ModStall), and has recently become in use at MET Norway. Although Overland and Modified Stallabrass are being used operationally, these algorithms have never been tested against real icing observations in the Barents Sea (Operational weather forecasters at MET Norway, Tromsø, 2014, pers. comm., March). In this paper the two algorithms are tested against a unique ship icing data set and the corresponding meteorological and oceanographical conditions from a severe icing case on the Norwegian Coast Guard vessel KV Nordkapp during a voyage late February 1987. In addition, adjustments of these two algorithms, and a third proposed algorithm with adjustments, are tested.

ICING THEORY AND ASSUMPTIONS

Icing on vessels in the ocean is usually divided into marine and atmospheric icing of which marine icing is assumed to be the most serious one. Figure 1 shows an overview of the marine sea-spray icing process. In the most common marine icing cases waves interact with a ship (or an offshore structure) and these collisions between the waves and the ship may generate sea spray. This spray can then be lofted by the airflow around the ship to higher elevations and freeze onto different parts of the ship. Turbulence in the airflow may bring sea water droplets to sheltered areas of the ship causing icing on the lee side of the ship. The theory of marine icing processes is detailed in Kulyakhtin (2014). Atmospheric icing results from supercooled fog, freezing rain/drizzle or snow when the temperature drops below 0°C (Stallabrass, 1980). The icing rate at a given position on a ship is calculated by taking into account the different heat fluxes involved in the icing process on a freezing surface from a given amount of spray delivered to the same surface. A thorough list of most fluxes involved in the freezing process is e.g. found in Jessup (1985). When only taking into account the most important fluxes, the heat equation is simplified to:

$$Q_f = Q_c + Q_e + Q_d \tag{1}$$

Eq. 1 shows that the energy released by freezing equals the convective cooling, the evaporative cooling and an additional term which represents the heating or cooling from the sea water to the freezing surface. The full definition of these heat fluxes is found in Table 1. In the current analysis conduction and radiation are neglected. Conductive heat flux is only significant in the beginning of a freezing process (Jessup, 1985) and as the calculations in this case are starting when the ice thickness is already 3 cm, conduction is not taken into account. Radiative heat flux is not considered important since the long-wave radiative heat flux is only 9% of Q_c under normal sea spray freezing conditions according to Kulyakhtin (2014), and the short wave radiative heat flux at 70°N in February is presumed to have little importance.

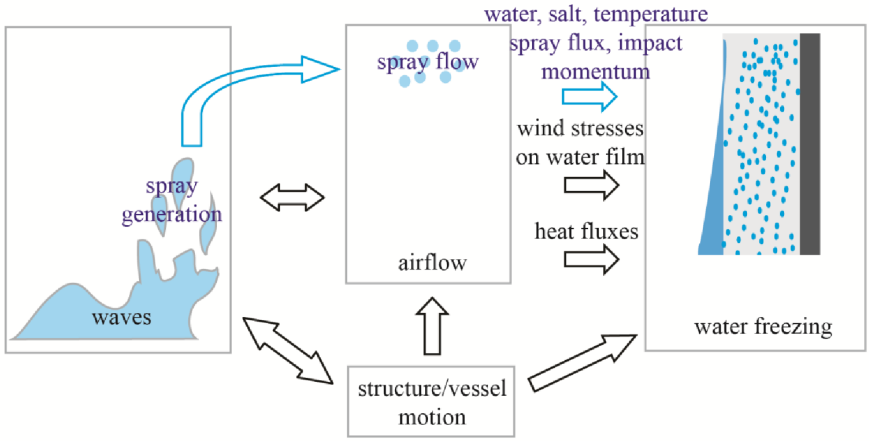

Figure 1: Overview of the marine icing process (Kulyakhtin, 2014).

ALGORITHMS USED IN CALCULATIONS

Overland algorithms (O1, O2, O3)
Overland (1990) (O1) and Overland et al. (1986) (O2) algorithms are based on a simplified solution of the heat equation (eq. 1) with assumptions as seen in Table 2. This will lead to a heat equation in the following form:

$$L_{fs}R_i = a_0 v(T_f - T_a) + \frac{c_w}{n} R_i (T_f - SST) \tag{2}$$

By rearranging eq. 2 and using $R_i = \rho_i \frac{dh}{dt}$ gives:

$$\begin{aligned} \frac{dh}{dt} &= \frac{\frac{a_0}{L_{fs}\rho_i} v(T_f - T_a)}{1 + \frac{c_w}{nL_{fs}}(SST - T_f)} \\ \frac{dh}{dt} &\propto Pr, \quad Pr = \frac{v(T_f - T_a)}{1 + \frac{c_w}{nL_{fs}}(SST - T_f)} \end{aligned} \tag{3}$$

Further Overland (1990) and Overland et al. (1986) used icing rate observations to find the best polynomial fit between $\frac{dh}{dt}$ (cm/h) and Pr, by assuming a constant freezing fraction, n. As a consequence whenever the convective heat flux is positive ($T_f > T_a$), freezing will occur and the spray flux will be 18 and 23 times larger than the ice accretion flux when using values for c_w and L_{fs} from Table 1 and $\Phi = \frac{c_w}{nL_{fs}} = 0.3$ from Overland (1990), and 0.4 from Overland et al. (1986). This means that there is always a sufficient amount of water available for freezing regardless of the sea state and the speed of the vessel. A consequence of this is that the spray flux is assumed to increase when the air temperature decreases, which is obviously unphysical.

An alternative Overland algorithm (O3) is also tested where one instead of setting n constant, tries to solve the heat equation directly by finding an expression for n. Since we do not have the exact formulation of the heat-transfer coefficient in Overland et al. (1986) and Overland (1990), we need to find a new expression for h_a. If we assume a linear dependence between the heat transfer coefficient (h_a) and wind speed (v) to follow the basic assumptions from Overland et al. (1986), we need to derive a new h_a from $h_a = \frac{Nuk_a}{D}$. An assumption of a linear dependence must result in a $Nu \propto Re$ and not $Nu \propto Re^{0.8}$ like in other algorithms assuming turbulent flow (e.g. Stallabrass (1980)). This would result in h_a being independent of the dimension size.

Modified Stallabrass algorithms (M1, M2, M3)
The ModStall algorithm (M1) uses the bases of an algorithm developed by Stallabrass (1980) with assumptions as seen in Table 2 and Henry (1995). The constant w_0 in the lwc formulation is taken from Zakrzewski (1986) and the mean icing rate is calculated between z = 3.5 to 9.0 m (every half meter). Instead of calculating S_b, M1 uses an experimental derived expression between T_s and T_f taken from Tabata et al. (1967). Two adjusted ModStall algorithms (M2, M3) were also tested. M2

Table 2: Overview of simplifications and major assumptions between the different algorithms. For M1, M2, M3, T1, T2, T3, T_d is found by solving a droplet cooling equation (DCE) taken from eq. B.11 in Stallabrass (1980)

Alg.	Simplifications	T_d	T_s	S_b	D	h_a	z	Δt	V_r	n	R_w	w_0	Time avg.
O1	Q_e negl.	SST	T_f	no	no	$K \times v$	no	no	no	0.057	$18 \times R_i$	no	no
O2	Q_e negl.	SST	T_f	no	no	$K \times v$	no	no	no	0.043	$23 \times R_i$	no	no
O3	Q_e negl.	SST	T_f	no	no	$62 \times v$	3.0-5.0 m	no	10 m/s	solved	$v \times lwc$	6.36×10^{-5}	no
M1	$L_{fs} = L_f$	DCE	$(1+n)T_f$	no	3m	$5.18 \times v^{0.8}$	3.5-9.0 m	11.25-v/4	10 m/s	solved	$v \times lwc$	6.1457×10^{-5}	no
M2	$L_{fs} = L_f$	DCE	$(1+n)T_f$	no	3m	$5.18 \times W_r^{0.8}$	3.0-5.0 m	11.25-W_r/4	From obs.	solved	$W_r \times lwc$	6.36×10^{-5}	no
M3	$L_{fs} = L_f$	DCE	$(1+n)T_f$	no	3m	$5.18 \times W_r^{0.8}$	3.0-5.0 m	$\tau + t_{dur}/2$	From obs.	solved	$W_r \times lwc \times t_{dur} N$	6.36×10^{-5}	yes
T1		DCE	Found from S_b	$\frac{S_w}{1-n\times(1-k^*)}$	4m	$4.85 \times W_r^{0.8}$	3.0-5.0 m	$\tau + t_{dur}/2$	From obs.	solved	$W_r E \times lwc \times t_{dur} N$	6.36×10^{-5}	yes
T2		DCE	$(1+n)T_f$	no	4m	$4.85 \times W_r^{0.8}$	3.0-5.0 m	$\tau + t_{dur}/2$	From obs.	solved	$W_r E \times lwc \times t_{dur} N$	6.36×10^{-5}	yes
T3		DCE	Found from S_b	$\frac{S_w}{1-n\times(1-k^*)}$	4m	$4.85 \times W_r^{0.8}$	3.0-5.0 m	$\tau + t_{dur}/2$	From obs.	solved	$W_r E \times lwc \times t_{dur} N$	Diff. form.	yes

uses z = 3.0 to 5.0 m according to the icing observations taken on KV Nordkapp, W_r instead of v, and V_r from the observations instead of a constant value of 10 m/s. In addition a slightly different w_0 was used according to a calculation error in Zakrzewski (1986) which is mentioned in Zakrzewski (1987). The constant was slightly changed further to 6.36×10^{-5} since the calculated V_r in Zakrzewski (1987) was found to be 11.1 m/s and not 11.01 m/s by using the same methods as Zakrzewski (1987). These minor constant corrections were not considered to have a large effect on the result.

M3 uses a different droplet cooling time, since it was found that the Δt in the other ModStall algorithms was much longer than in the original Stallabrass (1980) algorithm ($\Delta t = \tau$), which also results in a much lower T_d. On the other hand, using $\Delta t = \tau$, gave very short cooling time and too little icing. It was therefore considered that the Δt should be slightly longer than in the original Stallabrass (1980), and a new expression based on the time of flight of the droplets, τ, and the half time of the spray cloud residence time at a certain location of the ship was used ($t_{dur}/2$). The logic behind this is that if all of the droplets are launched from the sea surface at the same time, not all droplets will reach the freezing plate at the same time due to turbulence and droplets having different starting points and velocities after collision. To represent this time lag for some of the droplets, one can assume that the first droplets are carried to the freezing surface by time τ, and the latest arriving droplets will arrive at $\tau + t_{dur}$. The mean value of the sum of these two expressions are therefore seen as an average time for droplet cooling time, $\bar{\Delta t} = \tau + t_{dur}/2$. The total cloud residence time over the whole ship, $t_{durtotal}$, is taken from Lozowski et al. (2000) and used to find an expression for $t_{dur} = t_{durtotal} - \tau$ (see Table 1). In addition to this the spray flux was time-averaged by multiplying the spray cloud time at the certain position of the ship by ship-spray frequency. Zakrzewski (1987) has observed spray jet generation every second ship-wave encounter on a medium-sized fishing vessel (MFV), and Horjen (1990) uses a spray jet frequency with every 4th wave encounter on a large whaling vessel. But Zakrzewski (1986, 1987) also suggest that due to ship rolling, pitch, heave and resonance, it might probably be better to use an empirical derived expression for ship-spray frequency of an MFV based on t_{per} instead of using t_{per} directly. In the lack of better expressions for the ship-spray frequency for KV Nordkapp, the empirical expression for N from an MFV is used here.

Test model algorithms (T1, T2, T3)
A third model setup (T1) is also tested by trying to calculate a more accurate expression for the salinity effects. Brine movement is however neglected to avoid making the model too complex. This algorithm uses most of the same bases as M3. In addition it calculates E based on droplets of 2 mm size hitting a 4 m wide structure and uses h_a for D = 4 m according to the plate where the observations are taken. T_s is calculated from an expression for S_b taken from Makkonen (1987). An adjusted test model (T2) uses $T_s = (1+n)T_f$ instead of finding S_b. The last algorithm (T3) uses the same bases as T1, but uses a different expression for lwc:
$lwc = 1.3715 \times 10^{-3} \times H_s^{2.5} \exp(-0.55z)$ (Roebber and Mitten, 1987).

ICING EVENT DESCRIPTION

On the 26th February 1987 KV Nordkapp sailed from Tromsø towards the waters between Bjørnøya and Hopen, and went into a serious icing event with 110 tons of ice accumulating during a 17 hours period. The ice had accumulated from the deck railing all the way to the top of the wheel house as can be seen in Figure 2. The icing load was observed based on readings of the draft/ballast water. In addition 20 cm accumulated ice was recorded on a fixed position of the ship (Table 3). At 00z there was no icing observed. The next observation, 6 hours later, shows a total thickness of 3 cm. It is not clear at what time, during these first 6 hours, the icing started, so only the icing observed from 06z is considered in later icing calculations. From 06z and onwards the observations were taken every 3

hour and at 21z the ship was entering the ice cover, resulting in minimal sea spray, consistent with the preceding observations showing little or no ice increase. Ice accretion rates are also manually estimated by the observer in a code format of 0 to 4 (Table 3). Because it is not known from where on the ship this information is achieved or how the recorded accretion rate 1 (slow accretion) and 2 (fast accretion) should be interpreted in terms of cm/h, this information will not be used in the icing calculations. It is still worth noticing that the accretion rate is recorded as fast on 12z and 15z although the ice thickness had not increased on the position where the ice thickness measurements were taken.

(a) **(b)**

Figure 2: Icing on KV Nordkapp on the 27th February 1987, Barents Sea. a) Foreship and wheel house, b) starboard walkway and railing.

METOCEAN CONDITIONS

Two days before the voyage of KV Nordkapp, a low pressure system in the northern part of Russia, and a high pressure system east of Greenland (not shown) led to northerly winds sending cold air all the way over an ice covered northern Barents Sea to the ice-free southwestern Barents Sea, with the ice edge at latitudes as far south as Bjørnøya. The cold air flow went over relatively warm sea water and the air column became unstable, which led to convection and wintry showers. During the following days a synoptic low pressure developed southwest of Bjørnøya, which intensified and moved eastward into the eastern part of the ice free Barents Sea. During the 26th February, the low was almost stationary around 74°N, 30°E (Figure 3) sending cold winds from Bjørnøya to Northern Norway, west of its center. At the end of the day the low started to develop into a Polar Low. Nordeng and Rasmussen (1992) mention "a ship" about 200 km west of the center observing 30 m/s around 17z, which matches the violent storm observation from KV Nordkapp 26th February 18z strikingly well. This is the strongest wind observation recorded from this low.

Observations from KV Nordkapp are in general restricted information, but the Norwegian Coast Guard allowed publication of the data for scientific purposes (M. N. Jørgensen, Department manager Norwegian Coast Guard, 2014, pers. comm., April). To get more information about the data for the event, and to check the quality, the original handwritten observations were collected from an archive at the Forecasting Division of Western Norway, MET Norway, and compared with the electronically stored data at the climate database at MET Norway. The observed position and met-ocean data is seen in Figure 3 and Table 3. In addition, salinity, ocean depth and *SST* are derived from an ocean model hindcast archive with 4 km horizontal resolution (Lien et al., 2013). When comparing the observed *SST* with the model *SST*, only small differences were found (<1°C) indicating that the

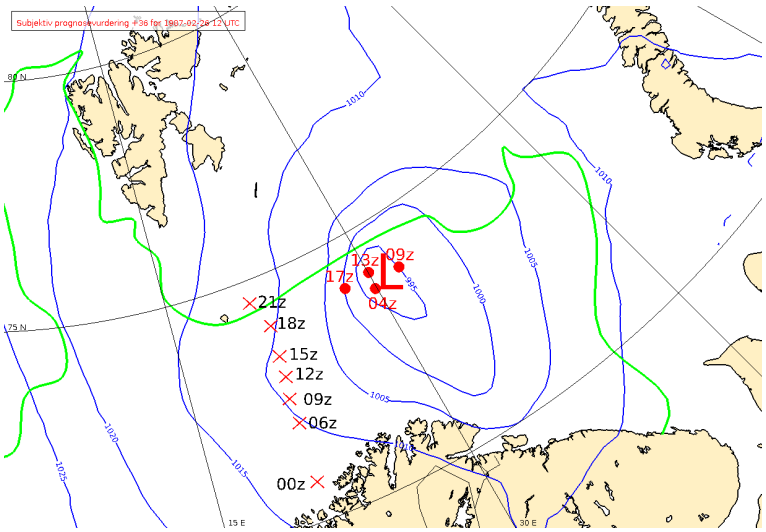

Figure 3: Synoptic situation at 26th February 1987, and the position of KV Nordkapp during the trip when Met-ocean observations were taken. The time of the observation is in UTC/Z (Universal time center/Zulu time). The green line is an approximate position of the ice edge taken from a Hirlam 10 km +06 hour prognosis at 26th February (Initial time 1987-02-26 06Z) and adjusted according to satellite data (NEODAAS/Dundee University,Nordeng and Rasmussen (1992)). The Hirlam 10 km is an atmospheric numerical weather prediction model with 10 km horizontal resolution and is taken from a hindcast archive provided by the NDP - Norwegian Deepwater Programme (Reistad et al., 2011). The MSLP analysis is shown in blue lines with 5 hPa contour interval. The MSLP field is derived from the Hirlam 10 km model, and adjusted according to MSLP from Synop observations at 12z. The red dots mark the approximate position of the low during the day according to satellite image information from 0428z, 0853z, 1243z and 1702z (NEODAAS/Dundee University,Nordeng and Rasmussen (1992))

measured cooling water temperature may be a good representation of the *SST*.

In general the ship went against 20-30 m/s winds from north-west and north with a maximum around 18z, corresponding well to the almost stationary low positioned at around 74°N, 30°E. The air temperature was below -12°C from 06z and the *SST* around +3-4°C. When reaching the ice edge at

Table 3: Observed Met-ocean and position data from KV Nordkapp 26th February 1987. Code values are taken from MET-Norway (1981).

Time	**00z**	**06z**	**09z**	**12z**	**15z**	**18z**	**21z**	**Comments**
Latitude	70.8	72.0	72.5	73.0	73.4	74.0	74.5	
Longitude	21.0	21.4	21.5	21.8	22.0	22.1	21.4	
h (cm)	x	3	10	10	10	15	20	Obs. thickness on a certain pos. on ship
Icing cause (code)	x	1	1	1	1	3	3	1 = sea spray, 2 = fog, 3 = sea spray + fog, 4 = freezing rain, 5 = sea spray + freezing rain, (MET-Norway, 1981)
Icing rate (code)	x	2	2	2	2	2	0	0 = no accretion, 1 = slow accretion, 2 = fast accretion, 3 = melt/breaking slowly, 4 = melt/breaking fast, (MET-Norway, 1981)
p (hPa)	1003.5	1009.3	1010.2	1008.8	1007.0	1005.1	1008.4	Observed pressure adjusted to sea level
DD (°)	330	345	340	340	340	350	360	Compass angle indicating direction wind is blowing from.
v (kt)	30	40	40	40	40	60	45	Read manually from the anemometer display. Observed in whole knots.
v (m/s)	15.4	20.6	20.6	20.6	20.6	30.9	23.2	Converted from knots to m/s by multiplying $\frac{1852}{3600}$
T_a (°C)	-5.1	-12.3	-12.8	-13.8	-16.8	-17.9	-21.5	
RH (%)	90.0	80.5	88.4	87.7	87.1	87.8	83.5	Taken from handwritten data.
Weather at obs. time (code)	86	86	73	85	85	86	86	73= moderate snow, 85 = light snow showers, 86 = moderate or heavy snow showers
Weather last 3-6 hrs 1 (code)	8	8	7	8	8	8	8	8 = showers
Weather last 3-6 hrs 2 (code)	8	8	4	7	8	4	4	7= snow or sleet, 4 = fog
Visibility (code)	95	95	94	94	94	91	94	90 = 0-50 m, 91 = 50-200 m, 92= 200-500 m, 93 = 500-1000 m, 94 = 1-2 km, 95 = 2-4 km
SST (°C)	3.2	4.1	4.2	3.9	3	2.6	-1.0	Measured in cooling water intake
SST from ocean model (°C)	3.7	4.2	3.8	3.0	2.5	2.2	-1.4	Taken from Nordic4km ocean model hindcast archive (Lien et al., 2013)
H_s (m)	3.0	7.5	5.5	5.5	5.5	5.0	0	Visually estimated in half meters, and here converted to whole meters.
P_w (s)	5	10	8	8	8	8	0	Visually estimated
S_w (ppt)	34.8	35.0	35.0	35.0	34.9	35.0	34.8	Taken from Nordic4km ocean model hindcast archive (Lien et al., 2013)
D_p (m)	234	348	332	430	441	448	132	Taken from Nordic4km ocean model hindcast archive (Lien et al., 2013)
c	7.8	15.6	12.5	12.5	12.5	12.5	0	Calculated from eq.5 p.8
λ (m)	39	156	100	100	100	100	0	Calculated from $\lambda = cP_w$

21z the air temperature dropped below -20°C and the *SST* went below 0°C. The wave height reached its maximum (7.5 m) in the beginning of the trip (06z). When sailing northwards the wave height decreased, even though the wind speed was the same or increasing. Actually the wave height reached its minimum value over open water when the wind was strongest at around 18z. However, at this point the ship was not far from the ice edge, and the fetch for building up high waves was much smaller than at 06z (Figure 3). During the whole trip there were snow or snow showers accompanied with fog, and the observed visibility varied from 50 m to 4 km.

The wave phase speed was calculated to find a relative speed between the waves and the boat. The general formula for the wave phase speed as a function of wave period and water depth is given as (eq. 7.41 Cohen and Kundu (2004)):

$$c = \frac{g}{2\pi} P_w \tanh \frac{2\pi D_p}{cP_w} \tag{4}$$

Since c is a function of $\tanh \frac{1}{c}$, this could be solved by an iterative process. But for $D_p >> \frac{1}{2} cP_w, \tanh \frac{2\pi D_p}{cP_w} \rightarrow 1$, deep water approximation is valid. By comparing the wave length ($\lambda = cP_w$) in Table 3 with the water depth from Nordic 4 km (Lien et al., 2013), it is seen that $D \sim$ 2-6λ, implying that c can be calculated according to:

$$c = \frac{g}{2\pi} P_w \tag{5}$$

SHIP, TRIP, ICING RATE AND SPEED DATA

The most important ship data (Table 4) is taken from the General Arrangement (GA). The length, width, draft and moulded depth is given directly in the GA. The height above sea level and the elevation of the wind and pressure measurement devices are based on measurements in the GA. The temperature and humidity are measured at the same location as the pressure.

Table 4: Ship data.

	Length	**Width**	**Draft**	**Moulded depth**	**Height ASL**	**Wind HASL**	**Pressure HASL**
Units in m	105.0	14.6	4.5	7.5	27.5	22.0	12.0

The icing measurements (Table 3) were taken at a fixed position on an almost vertical plate (85°tilt) going from the front deck to the canon deck (L. Kjøren 2014, Retired officer Norwegian coast guard, pers. comm., 4th November). From the bell on this plate to the depth of the ship, it is 12 m (Figure 4 a)). Since the draft of the ship is 4.5 m, the distance from the sea level to the bell is assumed to be 7.5 m. Spray flux algorithms in later calculations are based on Soviet MFV. According to Zakrzewski and Lozowski (1989) the freeboard of an MFV is 3.5 m, and z is calculated from deck level. It is therefore assumed that the bell is situated z = 4 m (7.5 m-3.5 m) above an assumed deck level of an MFV, and the icing is calculated as a mean value of the predicted ice thickness in an area around the bell from z = 3 to 5 m in the algorithms M2, M3, T1, T2 and T3. The width of this plate is measured to be 4 m which is taken into account in the Test model algorithms (Table 2). The distance from the central point of the plate to the outer edge of the hull varies from b = 6.1 m to a = 19.7 m (Figure 4 b)). If it is assumed that the edge is elliptical shaped with the midpoint of the plate as the center, the distance from the midpoint to the edge could be described as:

$$s = \frac{ab}{\sqrt{a^2 - \cos^2 \alpha (a^2 - b^2)}} \tag{6}$$

The distance s with α_c as input instead of α in eq. 6, s_r, is used to calculate the droplet flight time, τ, in the M3, T1, T2 and T3 algorithms (Table 1). To find the speed and direction of the boat during the

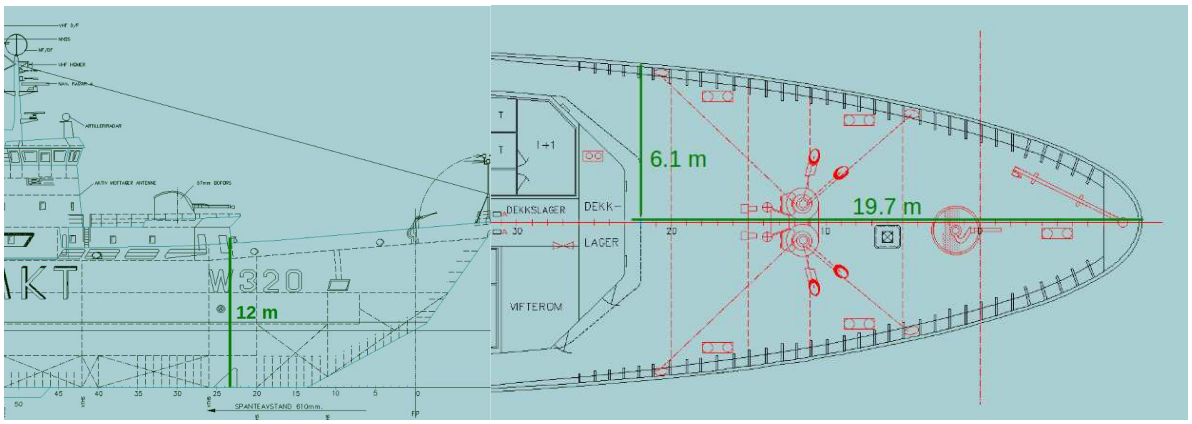

(a) **(b)**

Figure 4: Front part of KV Nordkapp taken from General Arrangement (provided by F. A. Melsbøe 2014, Chief engineer Norwegian coast guard, pers. comm., August). Distance is measured from GA. a) Side view, b) above view.

voyage, the mean speed and heading between the observation points are used. The distance between these points is calculated using the WGS84 coordinate system (Decker, 1986) and it is assumed that the ship is travelling with a constant heading, i.e along a rhumb line.

Observed icing rates are derived from the accumulated ice between the observation points every three hours from 06z to 21z. This will give a mean icing rate in the time interval between the observations (Table 5). This icing rate is compared with icing rates calculated from the different icing rate algorithms. It is chosen to first calculate the icing rate from the different algorithms at the start and the end points of the interval, and then find the mean icing rate as the mean value of these two numbers. Some of the algorithms need a relative speed between the ship and the waves, and the wind and the waves. Because only the wind direction is observed, it is assumed that the waves and the wind have the same direction. The angle and the relative speed between wind/waves and ship are then calculated at the start and end point of the time interval using the same ship speed and direction at the two points (Table 5).

Table 5: Trip data, icing rate, relative angle, relative wave and relative wind speed data in the time interval between the observations. It is assumed that the wind and waves are in the same direction. For convenience the heading (*Dir*) is defined in the same manner as the wind direction, i.e. 180° means a course from south to north.

Time	**06-09z**	**09-12z**	**12-15z**	**15-18z**	**18-21z**	**Comments**
Travelled distance (km)	55.9	56.7	45.1	67	59.7	Calculated from lat. and lon.
Dir (°)	183	190	188	183	159	Direction travelling from
v_s (m/s)	5.2	5.2	4.2	6.2	5.5	$vs = \frac{Distance}{Timedifference}$
Observed $\frac{dh}{dt}$ (cm/h)	2.3	0	0	1.7	1.7	
α start point	162	150	152	157	191	Rel. angle: $\alpha = DD - Dir$
α end point	157	150	152	167	201	
V_r start point	20.4	17.0	16.2	18.2	17.9	Rel. wave-boat speed: $V_r = c - v_s \cos(\alpha)$
V_r end point	17.2	17.0	16.2	18.5	5.2	
W_r start point	25.4	25.3	24.4	26.4	36.3	Rel. wind-boat speed: $W_r = \sqrt{v^2 + v_s^2 - 2v_s v\cos(\alpha)}$
W_r end point	25.4	25.3	24.4	37.0	28.3	

SIMULATION RESULTS

An overview over the most important results from icing calculations is seen in Figure 5 and Table 6. One should notice the extremely high icing rate calculated by the Overland algorithms. The O1 and O2 actually predict an icing rate above 100 cm/h at 21z, but since the ship now is inside the ice cover and the wave height is zero, the value is manually put to 0 to get a better comparison with the other algorithms. The mean value between 18z and 21z is therefore much lower than it otherwise would

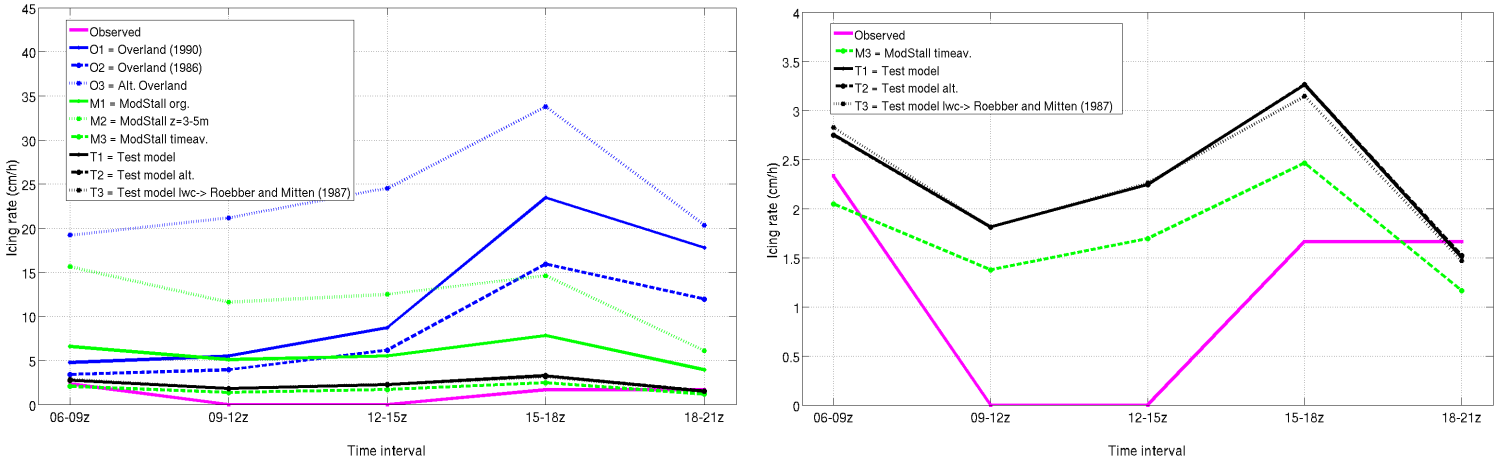

Figure 5: Icing rate calculated and observed. The three Overland algorithms (O1, O2, O3) are shown in blue colour, the three ModStall algorithms (M1, M2, M3) are shown in green colour and the three Test model algorithms (T1, T2, T3) are black.
a) Shows the observed icing rates and icing rates from all 9 algorithms.
b) Zoomed in view for icing rates below 4 cm/h which shows the observed icing rates together with the remaining 4 algorithms closest to the observed values.

have been. It is also seen that the O3 algorithm predicts an even higher icing rate than O1 and O2, especially in the beginning of the trip when the wave heights are high and the sea water relatively warm. The M1 and M2 are also giving very high sea-spray icing values. For the remaining 4 algorithms the range of the icing rate is more comparable to what is observed at the fixed position on KV Nordkapp (Figure 5 b). The effect of changing the droplet cooling time to something that is more similar to the droplet flight time, reduces the icing as seen when comparing the M3 algorithm with M2 and M1. Without time averaging the icing rate in the M3 algorithm was almost 0 (not shown). When applying more realistic treatment of the brine entrapment (Test models), the icing rate is slightly increased from the M3 algorithm. The use of a direct calculation of the brine salinity and the new freezing temperature (Makkonen, 1987), instead of using the more simplified expression from Tabata et al. (1967), does not seem to have a large effect (T2 compared to T1). A comparison of T1 and T3 shows that the *lwc* formulation of Zakrzewski (1987) gives almost the same results as using the *lwc* formulation of Roebber and Mitten (1987).

Table 6: Mean values of selected variables and total ice accumulation for the 9 different algorithms and the observations: The units are found in Table 1 except for R_w and R_i which uses units in g/m^2s, *lwc* which is shown in g/m^3 and n which is shown in %. n refers here to the fraction between the mean value of R_i and R_w and not to the mean value of the calculated n in the different algorithms. $\frac{\bar{dh}}{dt}$ is the mean from all intervals, while $\frac{\bar{dh}}{dt}_2$ is only taken from the intervals where it is observed an ice accretion. *Bias* (cm/h) and *MAE* (cm/h) is calculated according to the whole trip, while $Bias_2$ and MAE_2 is only calculated for the intervals with non-zero icing rate observed.

Variables	$\frac{\bar{dh}}{dt}$	*Bias*	*MAE*	T_d	Δt	*E*	h_a	*lwc*	R_w	R_i	*n*	T_s	$\sum h$	$\frac{dh}{dt}_2$	$Bias_2$	MAE_2
Observed	**1.1**												**17**	**1.9**		
O1	12	10.9	10.9	3.1	0	1	x	20.3	520	30	5.7	-1.9	181	15.3	13.4	13.4
O2	8.3	7.1	7.1	3.1	0	1	x	18.7	477	20	4.3	-1.9	124	10.4	8.5	8.5
O3	23.8	22.7	22.7	3.1	0	1	1419.4	3.8	85	59	69.2	-1.9	357	24.4	22.6	22.6
M1	5.8	4.7	4.7	-11.4	5.5	1	63.1	4.8	109	14	13.2	-2.4	87	6.1	4.2	4.2
M2	12.1	10.9	10.9	-9.4	4.3	1	73.8	11.9	329	30	9.1	-2.3	181	12.1	10.2	10.2
M3	1.7	0.6	0.9	-2.5	1.2	1	73.8	11.9	57	4	7.6	-2.1	26	1.9	0	0.5
T1	2.3	1.2	1.2	-2.5	1.2	0.96	69.2	12.1	56	6	10.2	-2.1	35	2.5	0.6	0.7
T2	2.3	1.2	1.2	-2.5	1.2	0.96	69.2	12.1	56	6	10.2	-2.2	35	2.5	0.6	0.7
T3	2.3	1.2	1.2	-2.5	1.2	0.96	69.2	11.3	54	6	10.5	-2.2	35	2.5	0.6	0.7

It is interesting to observe that the ice thickness remains constant from 09z to 15z, when all the algorithms predict a non-zero ice accretion. To be able to only look at the icing calculations in the period where it is an observed accretion, the *Bias* and *MAE* (Table 1) for the 3 time intervals (06-09z,15-18z and 18-21z) is also calculated and shown in Table 6. This seems to give a slight reduction of the positive *Bias* and *MAE* for the 4 low icing algorithms.

DISCUSSION

Why do the 5 first algorithms give so much more icing than the remaining 4 algorithms? Since the icing value of O1 and O2 is made through a third polynomial fit between a predictor with linear dependence of v and the continuous icing rate, the calculated rate has actually a cubic dependence of v (Table 10 Overland et al. (1986)). By taking a rough linear fit between the cubic expression of the predictor from 0 to 100 and the icing rate which has values of 0 to 7.5 cm/h, one can find that the heat transfer coefficient would approximately be $42 \times v$, if one assumes a linear dependence between icing rate (converted to m/s) and the predictor Pr in this range in O1 and O2. That is done by assuming that $dh/dt \approx K \times Pr$ (eq. 2), where $K = L_{fs}a_0/\rho_i$, and a_0 is then calculated to be 42. This is a somewhat lower a_0 than the O3 algorithm ($a_0 = 62$) taken from an assumed linear dependence between Nu and Re, but it still gives much higher values for h_a than the value of around $5 \times v^{0.8}$ that the other algorithms give. This very high heat transfer coefficient is partly compensated in O1 and O2 at high sea surface temperatures by assuming a very high spray flux (constant n), which makes the Q_d higher. Since the droplet temperature is put equal to the SST, this will always contribute to damping the cooling from the Q_c since SST at open ocean always is above its freezing temperature. When the n is not put to a constant as in the O3 algorithm, one can see that a lower spray flux does not compensate the high h_a to the same extent as in O1 and O2 (Figure 5).

For the M1 and M2 algorithms, the droplet cooling time is set relatively long. The result of this is that the Q_d term is directly contributing to even more icing, since the droplet temperature now is below the freezing point of the brine. When comparing the M2 with the M1 algorithm, it is also seen that the icing is heavily increased when calculating icing for lower levels (z = 3-5 m) and using relative wind speeds and observed relative wave-ship speed instead of a constant value of 10. Using wind speed and constant V_r as in the original ModStall (M1) is therefore partly masking the effect of assuming a long Δt which gives a low T_d and hence high icing rate.

Finally when comparing the sea spray algorithms with the observed mean icing rate on a certain position on KV Nordkapp, one makes several assumptions that also should be discussed:

- The observed mean icing rate at a fixed position on a ship is comparable to an instantaneous icing rate calculated from the end and the start point of the interval and then averaged. This was done since there are no realistic metocean data values available during the whole 3 hours, so a mean value is the best value one can get.

- The icing values measured at the vertical plate on KV Nordkapp represent the icing conditions in the current weather situation. As seen from table 3, there was also a measured icing rate visually estimated to be fast accretion although the manually measured thickness did not increase. The reason for this is unclear but wave washing or porous ice breaking off are possible reasons for this discrepancy. Nevertheless this indicates that the uncertainty in the measured icing values is high.

- The *lwc* formulation from a medium sized fishing vessel can be used as an expression for the *lwc* on KV Nordkapp. This was used since there are no other *lwc* formulation available for this kind of ship, and to make it easier to compare with algorithms that already use this *lwc* formulation.

- The visually estimated wave heights and wave periods are a good representation of the actual sea state. It is difficult to know how good the estimations from the observers are, but it has the advantage that it could possibly give different wave heights when wind speed and fetch are almost the same, which statistical relationships (Zakrzewski, 1987) could not give.

- A constant droplet size of 2 mm is fair to use. Choosing a different droplet size will affect both the droplet cooling time and hence how much the droplets are cooled. A 2 mm droplet size was chosen for easier comparison with the ModStall algorithms.

- The droplet cooling time is not easily chosen, and seems to affect the icing rate considerable. Droplets that hit different parts of a ship will probably also have different droplet temperatures. Also the same part of the ship could experience droplets with different temperatures. To find a good estimation of this remains as an open question.

- Both Arctic sea smoke and snow, could have contributed to icing in this case. In combination with sea spray icing the snow could easier stick to the already wetted surface. The snow in itself could also contribute to cooling and make the freezing point higher. Since the quantity of the water amounts from the fog and snow showers is not known, icing from these sources was neglected.

- The Overland algorithms could be used for calculating continuous icing rates. Overland (1991) defends the criticisms from Makkonen et al. (1991) that his algorithm should not be used for calculating continuous icing rate and only when forecasting categorical icing rate (light, moderate, severe). But Overland et al. (1986) use continuous icing rates when comparing his algorithm to others, and continuous icing rates gives the basis for categorical forecasting used operationally today (Operational weather forecasters at MET Norway, Tromsø, 2014, pers. comm., March).

CONCLUSIONS

Sea spray icing is a phenomena which is complex and difficult to forecast precisely where the uncertainty regarding different factors involved is high. The results from this KV Nordkapp voyage might not be applicable when looking into other icing cases. In spite of this uncertainty, when comparing both the *Bias* and *MAE* from all time intervals and the time intervals with an ice accretion in Table 6, two conclusions can be made:

1) It is difficult to distinguish any quality differences between the algorithms resulting in the lowest icing, indicating that taking into account salinity effects and using the *lwc* formulation from Roebber and Mitten (1987) instead of Zakrzewski (1987), does not increase the quality in icing rate prediction for this KV Nordkapp case.

2) The operational algorithms Overland and ModStall used in the Meteorogical society and its associates (O1, O2, O3, M1, M2) have much higher icing rates for the tested vertical plate on KV Nordkapp than all the other tested algorithms and the observed icing rates. The reason for this seems to be the large heat transfer coefficient with a linear dependence assumption in the Overland algorithms and a very long droplet cooling time in the ModStall algorithms. In fact when trying to calculate an overall ice thickness by using a constant icing rate in each of the time intervals, this will give ice thicknesses from 87 cm to 357 cm, when using these algorithms. This seems to be an unreasonably high value even though the observed ice thickness increase of 17 cm during these 15 hours is not a very accurate measure.

REFERENCES

Aksyutin, L. *Icing of ships (in Russian).* Leningrad, Sudostroyenije Publishers, 1979.

Bolton, D. The computation of equivalent potential temperature. *Monthly weather review*, 108(7): 1046–1053, 1980.

Cohen, I. and Kundu, P. *Fluid Mechanics*. Elsevier Science, 2004. ISBN 9780080470238.

Decker, B. L. World geodetic system 1984. Technical report, DTIC Document, 1986.

Ekeberg, O.-C. State-of-the-art on the marine icing models and observations. Techincal report (confidential) 2010-0745, DNV - Det Norske Veritas, 2010.

Henry, N. L. Forecasting vessel icing due to freezing spray in Canadian east coast waters. Part I: Model physics. Environment Canada, Newfoundland Weather Centre, 1995.

Horjen, I. *Numerical modelling of time-dependent marine icing, anti-icing and de-icing*. Doctoral thesis, NTH - Norges Tekniske Høgskole, 1990.

Jessup, R. G. *Forecast techniques for ice accretion on different types of marine structures, including ships, platforms and coastal facilities*. World Meteorlogical Organization, 1985.

Jørgensen, T. S. Ising på fiskefartøyer. Technical report, Fiskeritek. Forskningsinst., 1981.

Kachurin, L., Gashin, L., and Smirnov, I. Icing rate of small displacement fishing boats under various hydrometeorological conditions. (3), 1974.

Kulyakhtin, A. *Numerical Modelling and Experiments on Sea Spray Icing*. PhD thesis, NTNU - Norwegian University of Science and Technology, 2014.

Lien, V. S., Gusdal, Y., Albretsen, J., Melsom, A., and Vikebø, F. B. Evaluation of a Nordic Seas 4km numerical ocean model hindcast archive (SVIM), 1960-2011, 2013.

Lozowski, E. P., Szilder, K., and Makkonen, L. Computer simulation of marine ice accretion. *Philosophical Transactions of the Royal Society of London. Series A: Mathematical, Physical and Engineering Sciences*, 358(1776):2811–2845, 2000.

Makkonen, L. Salinity and growth rate of ice formed by sea spray. *Cold Regions Science and Technology*, 14(2):163 – 171, 1987. ISSN 0165-232X.

Makkonen, L. Solid fraction in dendritic solidification of a liquid. *Applied Physics Letters*, 96(9), 2010.

Makkonen, L., Brown, R. D., and Mitten, P. T. Comments on "Prediction of vessel icing for near-freezing sea temperatures". *Wea. Forecasting*, 6:565–567, 1991.

MET-Norway. Meteorological code for maritime stations (in Norwegian), 1981.

Moore, G. W. K. A climatology of vessel icing for the subpolar North Atlantic Ocean. *International Journal of Climatology*, 33(11):2495–2507, 2013. ISSN 1097-0088.

NEODAAS/Dundee University. NERC Earth Observation Data Acquisition and Analysis Service/Dundee University, 2014. URL `http://www.sat.dundee.ac.uk/`.

Nordeng, T. E. and Rasmussen, E. A. A most beautiful polar low. A case study of a polar low development in the Bear Island region. *Tellus A*, 44(2):81–99, 1992.

Overland, J. E. Prediction of vessel icing for near-freezing sea temperatures. *Wea. Forecasting*, 5: 62–77, 1990.

Overland, J. E. Reply. *Weather and Forecasting*, 6(4):568–570, 1991.

Overland, J. E., Pease, C. H., Preisendorfer, R. W., and Comiskey, A. L. Prediction of vessel icing. *J. Climate Appl. Meteor.*, 25:1793–1806, 1986.

Reistad, M., Breivik, Ø., Haakenstad, H., Aarnes, O. J., Furevik, B. R., and Bidlot, J.-R. A high-resolution hindcast of wind and waves for the North Sea, the Norwegian Sea, and the Barents Sea. *Journal of Geophysical Research: Oceans (1978–2012)*, 116(C5), 2011.

Roebber, P. and Mitten, P. *Modelling and measurement of icing in Canadian waters*. Atmospheric Environment Service, 1987.

Shellard, H. C. The meteorological aspects of ice accretion on ships. Technical Report 10, World Meteorological Organization, 1974. Marine Science Affairs Report.

Stallabrass, J. R. Trawler icing - A compilation of work done at N.R.C. Mechanical Engineering Report MD-56, National Research Council Canada, 1980.

Tabata, T., Iwata, S., Ono, N., and Hope, E. *Studies of ice accumulation on ships*. Directorate of

Scientific Information Services, DRB Canada, 1967.

Zakrzewski, W. P., Lozowski, E., and Muggeridge, D. Estimating the extent of the spraying zone on a sea-going ship. *Ocean Engineering*, 15(5):413 – 429, 1988. ISSN 0029-8018.

Zakrzewski, W. P. Icing of ships, part 1: Splashing a ship with spray. Technical report, NOAA - National Oceanic and Atmospheric Administration, 1986.

Zakrzewski, W. and Lozowski, E. *Soviet marine icing data*. Atmospheric Environment Service, Canadian Climate Centre, 1989.

Zakrzewski, W. Splashing a ship with collision-generated spray. *Cold Regions Science and Technology*, 14(1):65 – 83, 1987. ISSN 0165-232X.